Capture of interstellar objects in the Solar system

Jonathan Petersson

Lund Observatory
Lund University

2020-EXA164

Degree project of 15 higher education credits
June 2020

Supervisor: Daohai Li

Lund Observatory
Box 43
SE-221 00 Lund
Sweden

Abstract

Research on InterStellar Objects (ISOs) has been done for several decades, however, the first observed ISO in the Solar system was only recently discovered in 2017. It was named 1I/'Oumuamua and was only passing though the Solar system, but this may not be the case for all objects of its kind. For instance, one could gain a bound orbit around the Sun if the right amount of nudge is acquired when passing by a planet.

The purpose with this thesis is to determine the capture rate of interstellar objects in the Solar system and the orbital features of captured objects. This has been done by N-body simulations where we include the four giant planets Jupiter, Saturn, Uranus and Neptune, and ISOs flying towards the Solar system from random directions.

One set of simulations is done regarding how captures happen, e.g. whether encountering a planet is necessary or not. The results suggest that a close encounter with a planet is essential for a capture to happen.

The contribution on capture rate from each planet is also studied by doing separated simulations with that planet. Maybe a bit surprisingly, the capture rate is not additive in that the overall capture rate of the Solar system is lower than the sum of that of each planet, though still higher than any individual planet. We suspect the reason could lie in increased possibility for encounters with the planets, which can cause quick ejections.

Then we calculate the actual capture rate assuming a Maxwellian velocity distribution for the ISOs with a dispersion of 30 km/s, and the resulting volume capture rate is 0.0120(3) au^3/yr. Therefore, with a current estimate for number density of 0.1 au^{-3} for 'Oumuamua-like objects, we expect to capture 1200 objects per Myr. The orbit of captures are typically very eccentric with large semi-major axis. These captured objects may then encounter planets frequently, and as a result, get ejected from the Solar system within a few Myr.

Acknowledgements

I would like to express my deep gratitude to my supervisor, Daohai Li, for his valuable guidance throughout this project. Without it, this project would not have been possible.

I would also like to thank my fellow bachelor students who I have worked with, for their support and meaningful discussions.

Finally, I would like to thank my family and friends, for their support throughout this entire project.

Populärvetenskaplig beskrivning

Forskning inom interstellära objekt, det vill säga objekt som har sitt ursprung utanför vårt solsystem, har pågått under decennier, men det var inte förrän 2017 som det första interstellära objektet i solsystemet upptäcktes. Det fick namnet 1I/'Oumuamua och skapade ett stort intresse både inom forskarvärlden och hos allmänheten. Två år senare, 2019, upptäcktes det andra och senaste interstellära objektet i solsystemet, som fick namnet 2I/Borisov. Både 'Oumuamua och Borsiov har och kommer däremot bara att passera solsystem under deras resa genom rymden. Den fråga man kan ställa sig då är hur stor sannolikheten är att ett interstellärt objekt istället fångas upp av solsystemet och hamnar i en stabil omloppsbana runt solen?

Syftet med detta projektet är att studera hur frekvent interstellära objekt fångas upp av solsystemet och undersöka hur en typisk omloppsbana ser ut för ett fångat interstellärt objekt. Detta genomförs med hjälp av simuleringar där vi följer utvecklingen för miljontals interstellära objekt som genereras jämt över en sfär som omger solsystemet, och där varje objekts hastighetsriktning är slumpvalt riktat inåt mot solsystemet.

De planeter som vi inkluderar i vår studie är de fyra yttre planeterna, Jupiter, Saturnus, Uranus och Neptunus. Hur mycket varje planet påverkar frekvensen av fångade interstellära objekt kommer även att analyseras. Två mindre studier kommer även att genomföras, där den ena handlar om hur interstellära objekt fångas upp, t.ex. om en nära interaktion med en planet är nödvändig, medan den andra gäller vad som sker med fångade interstellära objekt på lång sikt, t.ex. om de slungas åter ut i yttre rymden.

Upptäckterna av 'Oumuamua och Borisov, har bidragit med mycket ny kunskap, men det finns fortfarande delar inom området där vi vet mindre. Ett av dem är just frekvensen av interstellära objekt som fångas upp av solsystemet, som i nuläget det bara finns en studie på. Det är därför viktigt att bidra med mer kunskap som potentiellt kan driva forskning inom interstellära objekt framåt.

Contents

List of Figures

List of Tables

Chapter 1

Introduction

The first interstellar object (ISO) in the Solar system was observed on 19 October 2017 (Meech et al. 2017). The object was named 1I/'Oumuamua and its discovery sparked interest in both the scientific community and the general public. During the limited time period for observations, new and deeper knowledge about ISOs was obtained. In 2019, another ISO was discovered; it was named 2I/Borisov and will hopefully also contribute with more knowledge regarding ISOs (Jewitt and Luu 2019).

The orbit of 'Oumuamua was identified as hyperbolic (Meech et al. 2017), which means that it was only passing though the Solar system. However, when an ISO is traversing the Solar system, there is a possibility that it encounter a planet. The deflection caused by the encounter may change the object's orbit to be bound to the Solar system; the object is now considered captured. With this second possible outcome in mind, the question that then arises is how likely a capture of an ISO is to happen? This leads us to the purpose of this thesis: what is the capture rate of ISOs in the Solar system and what are the orbital features of the captured objects?

We are going to use extensive N-body simulations to assess these questions. There, we adopt a model where the Solar system is comprised of the four giant planets, Jupiter, Saturn, Uranus and Neptune, and the ISOs are approaching the Solar system from random directions. However, we first do a case study where we simulate the capture under the effect of only one planet. Doing so for the previously mentioned planets, the contribution of each is analysed. Along the way, we study how a capture happen, e.g., whether encountering a planet is needed. Then in a second step, we consider all four planets and derive a capture rate and look into the orbits of the captures. We also take a look at the long-term evolution for captured objects, e.g. if it is possible that a captured ISO can get ejected back into interstellar space.

A short discussion on 'Oumuamua and particularly on its origin is presented in section 1.1. Then, we discuss general three-body encounter in section 1.2 and the latest research regarding capture of ISOs in section 1.3. In chapter 2, we explain how the simulations are performed, e.g., how the initial conditions are created and how the statistics are calculated. The results on each planets contribution to the capture rate are presented in chapter 3. In chapter 4, the full results, i.e., the capture rate for the Solar system, are presented, and in

chapter 5 we take a look at the long-term evolution of captured ISOs. Finally, in chapter 6, we discuss further implications and present the conclusions.

1.1 'Oumuamua

As mentioned earlier, the discovery of 'Oumuamua sparked great interest in the scientific community, resulting in numerous research articles. The most important discoveries have been summarised by 'Oumuamua international space science institute (ISSI) team et al. ('Oumuamua ISSI Team et al. 2019) and we discuss some of these below. First, let us begin what was believed about ISOs before 'Oumuamua was discovered. It was predicted that the first observed ISO should be an active comet (McGlynn and Chapman 1989), which was mainly based on the fact that an active comet is much brighter than an asteroidal object, and therefore easier to detect, but also based on the expected similarity between ISOs and objects in the Oort cloud. Most objects in the Oort cloud were believed to be long-period comets that becomes active when they approach the Sun. It was therefore reasonable to assume that the first ISO should have the same morphology.

Having said that, the discovery of 'Oumuamua came as a surprise, since it was discovered that it is not an active comet (Meech et al. 2017; Trilling et al. 2018). Instead, it was found that the size of 'Oumuamua is in the 100 m range (compared to the kilometre-scale for long-period comets) and no sign of "cometary" activity was detected. However, non-gravitational acceleration was observed, since a gravity-only orbit did not make a perfect fit to the observations (Micheli et al. 2018). This implies that 'Oumuamua could have had some sort of mass loss that was not detected. Regarding the similarity between ISOs and the Oort cloud, nowadays, it is known that the Oort cloud also consists of a large number of inactive or weakly active objects (Meech et al. 2016). This means that if the assumption that objects in the Oort cloud are similar to ISOs, the spatial density of ISOs is higher than original predictions.

To better understand the density of ISOs, the origin of these objects has to be understood. 'Oumuamua ISSI Team et al. (2019) mentions this briefly and states that 'Oumuamua was most likely born as a planetary building block, a planetesimal, around a young star in a gas-dominated protoplanetary disk. There have also been observations which shows that around 20% of stars slightly older than the Sun, still have outer planetesimals. These reservoirs of planetesimals, that are capable of being dynamically ejected by nearby stars, could potentially be a source of ISOs. However, it is also very likely that 'Oumuamua and many other ISOs are already ejected during planetary system formation, where a significant number of planetesimals are ejected out from their birth system.

One mechanism that can cause a planetesimal to be ejected, is gravitational interaction with nearby stars, which gets significantly larger if the object gets too far out from its host star. Another example is interactions with giant planets in the system itself, where a close encounter can cause an ejection (Raymond et al. 2010). A third example is regarding binary systems, where if a planetesimal travels within a critical distance to the binary, it gets ejected (Jackson et al. 2018).

Regarding the number density of ISOs, it has been estimated[1] that there are 0.1 au^{-3} ISOs (in the same size as 'Oumuamua or larger) in interstellar space (Meech et al. 2017). This estimate was done with the observed absolute magnitude (22.4) of 'Oumuamua and current sky-survey detection limits.

Regarding the trajectory of 'Oumuamua, it was exactly what was excepted for detectable ISOs. The orbital elements for 'Oumuamua that were found during the observations, can be seen in table 1.1. These values agree well with the predicted distribution of values for detectable ISOs (Engelhardt et al. 2017), that was published only eight months before 'Oumuamua was discovered.

Table 1.1: Table with dynamical properties for 'Oumuamua ('Oumuamua ISSI Team et al. 2019; JPL's Solar System Dynamics group 2017).

Dynamical properties		Value
Eccentricity	e	1.20113 ± 0.000002
Semi-major axis	a(au)	-1.2723 ± 0.0001
Perihelion distance	q(au)	0.255912 ± 0.000007
Inclination	$i(^\circ)$	122.7417 ± 0.0003
Incoming velocity	v_∞(km/s)	26.4204 ± 0.0019

Other interesting features of 'Oumuamua that is highlighted by 'Oumuamua ISSI Team et al. (2019) is its shape, which was determined to be either a narrow elongated-ellipsoid shape or a shape more similar to a flattened oval. This unusually elongated shape can be used as an explanation for the observed short-term brightness variations that were detected during its passage through the Solar system. Having said that, an explanation for the shape itself still remains as an open question.

1.2 Three-body capture

One field of study that can be helpful in understanding capture of ISOs, is capture of free-floating planets by planetary systems. Free-floating planets are planets that in some way have been ejected out from their birth system and are therefore no longer bound to a star. These objects can then interact with other stars and planetary systems, which can result in a capture of the free-floating planet. The capture rate for these objects has been studied with three-body simulations by Goulinski and Ribak (2017), and these simulations can in many cases be applied to those for ISOs, with only a few adjustments.

The main difference between capture of free-floating planets and ISOs, is the difference in mass, but other than that, the dynamics are practically the same. In the study by Goulinski and Ribak (2017), three-body scattering events of a Jupiter-mass free-floater

[1]This number density is based on only one object ('Oumuamua), and it is therefore a fairly large uncertainty in this estimate.

with a Sun-Jupiter system are simulated. Three-body simulations will also be done in this thesis, but instead with ISOs and somewhat different methodology. In their simulations, different masses, velocities, and inclination angles are chosen for the free-floating planet, and the three different outcomes that are possible are, flyby, capture and exchange. In a flyby, the total energy remains positive, which means that the free-floating planet do not remain in the system, while in a capture, the total energy becomes negative, causing the free-floating to be bound the system. An exchange is when the free-floating planet 'replaces' the already bound planet, however, in the case of ISOs, only flyby and capture are possible.

The results from Goulinski and Ribak (2017) shows that a majority of the captures end up with a very eccentric orbit, and that there is a relation between semi-major axis and eccentricity, such that larger semi-major axis results in higher eccentricity. They also show relations on how the capture probability depends on initial velocity and inclination angle of the free-floating planet, which was done by generating free-floating planets with different initial velocities and inclination angles to the star-planet system. They found that the capture probability appears to decrease with higher initial velocity, while it increases towards a inclination angle of 90° (which from their definition corresponds to the star-planet orbital plane). Goulinski and Ribak (2017) studied also how the capture probability depends on the mass of the free-floating planet. They did this by varying the mass for the free-floating planet between 10^{-4} and 10^{2} Jupiter masses, and they found that the probability for capture increases with mass. This means that low-velocity free-floating planets with large mass (compared to Jupiter) that travel in the same plane as the planetary system, has the highest probability to be captured.

1.3 Capture of interstellar objects

The only work we know of regarding capture of ISOs in a gas-free environment, is that by Hands and Dehnen (2020). More precisely, they studied if ISOs could potentially be a source of long-period comets ($P > 200$ yr) in a Sun-Jupiter system[2]. Regarding the efficiency for capture of ISOs, they mention that captures of ISOs are efficient when they interact with primordial protoplanetary gas discs, but, due to the relatively short lifetime of these gas discs (~ 10 Myr), there is much more time for ISOs to be captured purely by gravitational dynamics. However, this does not exclude the possible importance of ISOs in formation of planets in protoplanetary discs. It is currently under debate if ISOs have a significant role in planet formation (e.g. Pfalzner and Bannister (2019)).

Coming back to the model by Hands and Dehnen (2020), in each simulation, 10^5 ISOs are modelled, which in the end results in a total of 404,800,000 simulated ISOs. The ISOs' initial positions were generated uniformly such that they form a spherical shell with a radius of 800 au from the barycentre of the Sun-Jupiter system. The relation that was

[2]The most popular theory for long-period comets is that they originally were scattered outward from the Solar system to the Oort cloud, where they can be scattered again by passing stars, back into the Solar system.

used to generate position- and velocity vectors was: $\boldsymbol{r}(t) = \boldsymbol{b} + t\boldsymbol{v}_\infty$, where $\boldsymbol{b}$ is the impact parameter. The maximum velocity at infinity of the ISOs was set to 12 km/s and the maximum impact parameter was set according to the following condition:

$$b \leq b_{\max} = B/v_\infty \quad \text{with} \quad B = 180 \text{ au km/s}. \tag{1.1}$$

The reasons for these restrictions on velocity and impact parameter is motivated by the fact that capture of ISOs decreases with both higher velocity and larger impact parameter. By having these restrictions, and neglecting the small number of ISOs that are captured at high velocities and large impact parameters, the computational cost is significantly reduced. Each simulation is run for 2000 years, such that the ISO with lowest velocity can complete its passage through the Solar system.

With these simulations, they found a volume capture rate of 0.051 $\text{au}^3\text{yr}^{-1}$ (assuming ISOs follow the local stellar velocity distribution). The volume capture rate is defined as the capture rate (number of captures per year) divided by the number density (number of ISOs per volume). With this, they could estimate a capture rate of $\simeq 10^4$ Myr^{-1} for 'Oumuamua-like rocks, using a number density with upper limit of 0.2 au^{-3}. They also found the capture rates of $\simeq 12$ Myr^{-1} for $\gtrsim$ 1km sized comets and $\simeq 1200$ Myr^{-1} for $\gtrsim$ 1km sized asteroids, which has a number density 100 times more abundant compared to the comet sized ISO, that has a number density of 2.4×10^{-4} au^{-3} (estimated by years of non-detections).

Hands and Dehnen (2020) also found that there is a higher probability of capture for objects that are in the same plane as Jupiter. This is because ISOs then have more opportunities to encounter Jupiter during their travel through the Solar system, and therefore get captured. Another observation is that the preferred velocity v_∞, for capture is $\simeq 0.6$ km/s, and that the probability for capture steadily decreases towards 12 km/s. It is therefore not surprising that neither 'Oumuamua nor Borisov, ended up captured, due to their relatively high velocities of 26 km/s and 32 km/s respectively.

One conclusion from Hands and Dehnen (2020), essential for this thesis, is that only a small fraction of ISOs gets captured, due to the preferred low-velocity for capture. They also briefly mention the possibility for captured ISOs with long periods to get ejected out from the Solar system by weak interactions with Jupiter. This effect has a timescale of 10 Myr and will briefly be studied in this thesis.

Without presenting any detailed simulations, they also highlight the possible importance of Saturn, Uranus and Neptune at $v_\infty \lesssim 0.5$ km/s, with indications of a forthcoming paper, which is not yet available. The purpose with this thesis is therefore to determine the possible contributions from the three other planets to the capture rate, but also to see if a somewhat different methodology, can result in a similar capture rate to that by Hands and Dehnen (2020). A capture rate for the Solar system where Jupiter, Saturn, Uranus and Neptune are taken into account, has been derived by Li (2019 personal communication). The result differs from that by Hands and Dehnen (2020), which justifies the importance with more results regarding the capture rate of ISOs in the Solar system.

Chapter 2

Numerical method

2.1 Initial conditions

To perform simulations with interstellar objects (ISOs), one has to first generate initial conditions, consisting of position and velocity vectors. Starting with initial position, we generate ISOs, such that they form a uniformly spherical shell around the Sun, at a radius of 10,000 au. Regarding the initial velocity, we generate ISOs with a velocity at infinity between 0.05 - 16.0 km/s. This velocity interval is then separated into 4 regions, each with different step size in velocity dv. The different regions and the respective step size can be seen in Tab.2.1. With this set up, a total of 25 different values for the velocity at infinity will be simulated. Generally, we want that d$v < v$, but, at the same time, we expect the probability for capture to decrease with higher velocity. It is therefore more efficient (in computational power) to increase dv with v, then to keep the same step size for all velocities. We are also more interested in ISOs with lower velocities, since this is where we expect the additional planets to have most significant impact on the capture rate, as suggested by Hands and Dehnen (2020).

Table 2.1: The four regions between 0.05 - 16.0 km/s and respective step size in velocity.

	0.05 - 0.5 km/s:	0.6 - 1.0 km/s:	2.0 - 6.0 km/s:	8.0 - 16.0 km/s:
Step size dv:	0.05 km/s	0.1 km/s	1.0 km/s	2.0 km/s

The velocity at infinity is defined as the relative velocity between the ISO and the Sun, when the ISO is infinitely far away. It is therefore not the same at the real velocity, which is instead used when generating initial conditions. The real initial velocity at 10,000 au, can be calculated through conservation of energy (Goulinski and Ribak 2017):

$$v = \sqrt{v_\infty^2 + \frac{2Gm}{r}}, \tag{2.1}$$

where we assume m to be the mass of the Sun, r is the distance to the Sun, G is the gravitational constant and v_∞ is the velocity at infinity.

Saving computational power is always beneficial, and we therefore generate velocity vectors such that the ISO flies by the Solar system at a significant close distance. This can be done with the help of gravitational focusing and the so called impact parameter. Gravitational focusing is an effect where a massive object can gravitationally focus other bodies towards it. The impact parameter is then defined as the perpendicular distance between the trajectory of one object and another, or the centre of a gravitational field, where the later is the case in this project.

Assuming that the mass of the Sun is much larger than the mass of the bound planet(s), and that the trajectory of the ISO behaves like a test-particle, the impact parameter can be calculated in the following way (Goulinski and Ribak 2017):

$$b^2 = r_{\min}^2 \left(1 + \frac{2Gm}{v_\infty^2 r_{\min}}\right), \tag{2.2}$$

where $r_{\min}$ is the closest approach between the ISO and the Solar system barycentre. We assume there is a maximum $r_{\min}$ (we think of it as the radius of the Solar system) beyond which the ISO will not be affected by the planet(s); then in accordance, there is a maximum impact parameter $b_{\max}$. The maximum impact parameter can be calculated using Eq. 2.2, and assigning $r_{\min}$ to be the radius of the Solar system. By generating an ISO, such that $b \leq b_{\max}$, we guarantee that there will be a "collision" between the ISO and the Solar system, so that the ISO will have the possibility to interact with the planet(s).

The specific value for $r_{\min}$ is varied between 100 au to 50 au, depending on simulation and velocity at infinity. In chapter 3 and 4, where the results regarding the simulations are presented, what value $r_{\min}$ has for each simulation is also presented and motivated.

An illustration that shows how the impact parameter is defined can be seen in Fig. 2.1. The angle α in Fig. 2.1, can be calculated with trigonometry

$$\alpha = \arcsin\left(\frac{b}{p}\right), \tag{2.3}$$

where p is the position vector for the ISO ($|p| = 10,000$ au). A velocity vector that has an angle $0 \leq \alpha \leq \alpha_{\max}$, will result in the ISO falling into the Solar system. The maximum angle $\alpha_{\max}$ can be calculated by replacing b with $b_{\max}$, in Eq. 2.3.

So far, we have generated initial positions and velocities w.r.t. the Sun. In reality, the ISO will gravitationally focus towards the barycentre of the Solar system, not the centre of the Sun. We therefore calculate the effect the four giant planets Jupiter, Saturn, Uranus and Neptune have on the Sun, and add this contribution of position and velocity to the ISO.

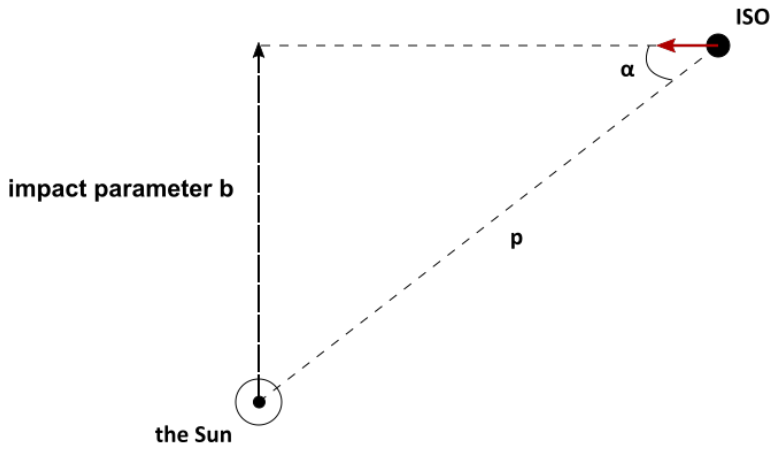

Figure 2.1: An illustration showing how the impact parameter b is defined. The angle α, which is used for generating velocity vectors, is also illustrated.

2.2 MERCURY

An N-body integrator propagates a system of objects, governed by Newtonian gravity. While many integration schemes exists, we demonstrate the basic idea with the simplest one, the Euler method. Let's assume a object is travelling along the x-axis. We then have the following ordinary differential equation (ODE) that describes the evolution of velocity

$$\frac{\mathrm{d}x}{\mathrm{d}t} = \dot{x} = f(x). \tag{2.4}$$

Given the initial value $x(t = 0) = x_0$, and if the time step δt is sufficiently small, we have that

$$x(t = \delta t) \approx x_0 + \delta t \cdot f(x_0), \quad \Longrightarrow \quad \begin{aligned} x_1 &\approx x_0 + \delta t \cdot f(x_0), \\ x_2 &\approx x_1 + \delta t \cdot f(x_1), \\ &\dots \end{aligned} \tag{2.5}$$

From this, we can see that the motion of the object can be described as a sum of small motions in time steps of δt. In our case, the motion of objects are calculated using Newton's law of gravitation, and for a system with N number of bodies, the resulting acceleration for body j ($j = 1, ..., N$) is therefore

$$\ddot{\boldsymbol{r}}_j = \sum_{i=1, i\neq j}^{i=N} \frac{G m_i (\boldsymbol{r}_i - \boldsymbol{r}_j)}{|\boldsymbol{r}_i - \boldsymbol{r}_j|^3}. \tag{2.6}$$

The N-body integrator that is chosen for the simulations in this project is MERCURY (version 6), written by Chambers (1999). MERCURY is designed to calculate the orbital evolution of objects that are moving in a gravitational field of a large central body, e.g. the Sun. One of the main features of MERCURY is also that it allows accurate calculations for close encounters between massive bodies.

MERCURY includes a variety of N-body algorithms, and the one used in this project is the so called general Bulirsch-Stoer algorithm. One feature of this algorithm is that once the error tolerance is set, it will choose its own timesteps in order to maintain the desired accuracy. Bulirsch-Stoer is also one of the more reliable algorithms for close encounters between objects.

Another feature of MERCURY that is useful in this project is that objects can be separated into two categories, Big- and Small body. A Big body is allowed to interact with other Big- and Small bodies, while a Small body only is allowed to interact with Big bodies, not with other Small bodies. This makes it possible to run simulations with thousands of Small bodies at the same time, since they do not affect each other. In this project, the planets are therefore assigned as Big bodies, while the ISOs instead are treated as Small bodies. All objects are also assumed to be point masses, and no collisions are allowed.

2.3 Calculating capture rate

We calculate the cross section for capture in the following way (McMillan and Hut 1996):

$$\sigma = \pi b_{\max}^2 P. \tag{2.7}$$

where σ is the capture cross section and P the fraction of interactions that resulted in a capture. The cross section can be described as the probability that a specific process will take place within a specific area.

The cross section can then be used to calculate the capture rate (Goulinski and Ribak 2017). Assuming a homogeneous flux of ISOs, with given relative velocity v, number density n and relative velocity distribution $f_{\mathcal{S}}$, with given relative velocity dispersion $\mathcal{S}$, the total capture rate can be calculated according to

$$R = \int n v \sigma(v) f_{\mathcal{S}}(v) \mathrm{d}v. \tag{2.8}$$

However, due to different number densities for different types of ISOs, the volume capture rate Q, can instead be used. This can be calculated by dividing the capture rate by the number density

$$Q = \frac{R}{n}. \tag{2.9}$$

Chapter 3

One-planet simulations

3.1 Capture rate comparison

Five simulations regarding each planet's contribution to the capture rate is carried out. For each of the four planets, a set of simulations is performed and in addition to these four, in a fifth, we consider all planets. In each simulation, the velocity at infinity is fixed at 0.05 km/s, and 100,000 interstellar objects (ISOs) are simulated. The integration time is 100,000 years, which is enough for the ISO to reach the Solar system, and to either pass through or get captured.

When the initial conditions for the ISOs are generated, the radius of the Solar system ($r_{\min}$ in Eq. 2.2) is set to 100 au, and the impact parameter corresponding to this value is $b_{\max}$. Test simulations have been done which shows that all captured ISOs have an impact parameter $\lesssim 0.9 b_{\max}$. This ensures that no captures are missed due to limited impact parameter, and our choice for the Solar system radius ($r_{\min}$) is therefore sufficient.

For an ISO to be considered captured, it has to fulfil two conditions. The first is that the eccentricity is $e < 1$ (which means that the ISO has an elliptical orbit), and the second condition is that the semi-major axis is $a \leq 6.5 \times 10^4$ au. The reason for this specific limit, is that it has been shown that at this distance, a large majority of objects become unbound to the Solar system (Correa-Otto and Calandra 2019). With these conditions on eccentricity and semi-major axis, the fraction of ISOs captured can be calculated and an error can be estimated using a method called Bootstrap. A brief explanation on how Bootstrap works can be read in appendix A.

When the fraction of captured ISOs are estimated, the cross section for capture (Eq. 2.7) can be calculated. With the cross section, the volume capture rate is determined using Eq. 2.8 and 2.9. The result from each simulation can be seen in Tab. 3.1, which presents the fraction of objects captured, cross section and volume capture rate. The result is also visualised in Fig. 3.1.

In Fig. 3.1, we can see that Jupiter and Saturn both results in similar volume capture rate, with Saturn slightly higher than Jupiter. We can also see that the volume capture rate for Uranus and Neptune are very similar and significantly smaller than those for Jupiter

and Saturn. The simulation that results in highest volume capture rate is the one with all planets included. However, it can be seen that the contribution from each planet is not additive. Neither is the fraction of objects captured or cross section, which can be seen in Tab. 3.1. We suspect the reason could be that the captured objects may be ejected more quickly when all planets are considered, since then there is a higher probability for close encounters. This will later be more discussed in chapter 6.

Table 3.1: Table with values for the per cent of objects captured, cross section and volume capture rate.

Planet(s) included in simulation	Per cent of objects captured	Cross section σ [au^2]	Volume capture rate Q [10^{-5}au^3/yr]
Jupiter	4.53(7)%	141790(2164)	1.289(20)
Saturn	5.02(7)%	157132(2194)	1.428(20)
Uranus	0.79(3)%	24824.8(846.8)	0.226(8)
Neptune	0.71(3)%	22122.2(819.3)	0.201(7)
All of the above	5.88(7)%	184038(2235)	1.673(20)

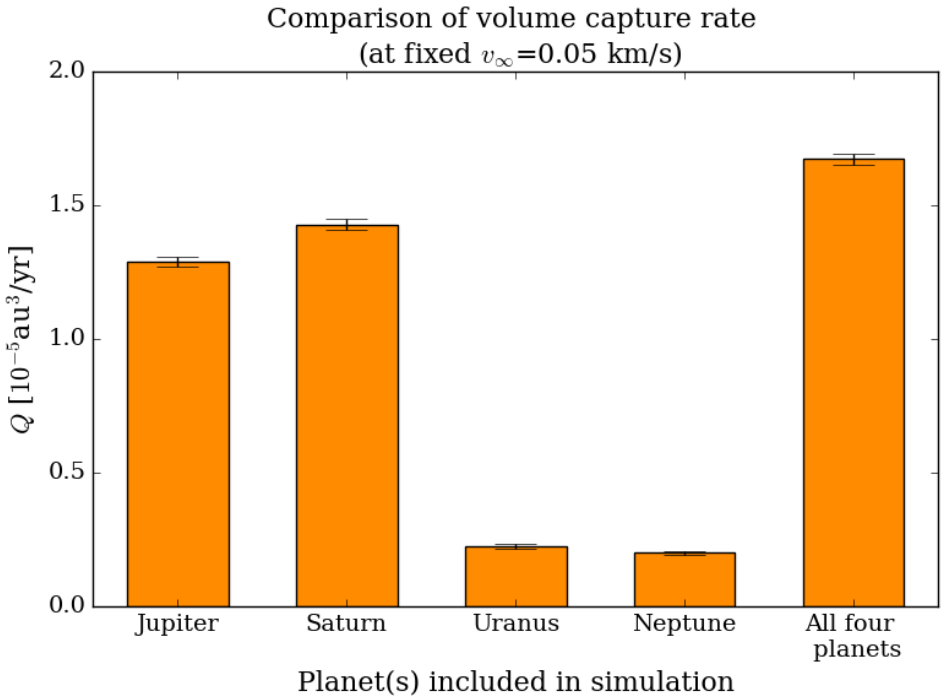

Figure 3.1: Visualisation of the difference in volume capture rate, depending on which planet(s) are included in the simulation.

Comparison of orbital features for the captured ISOs between the simulations can be seen in Fig. 3.2 and 3.3. In Fig. 3.2, we can see the relation between inclination angle and semi-major axis for captured ISOs for each simulation (the simulation with all planets included is called Solar system). The empirical cumulative distribution function (ECDF) for the inclination angle, is also shown. From Fig. 3.2, we can see an asymmetry in all simulations, where there are more captured ISOs with a inclination angle $i < 90°$. This implies that there are more captured ISOs with prograde orbit. An possible explanation for this could be that for prograde orbits, the ISO is travelling in the same direction as the planet, causing the relative velocity between the two to be smaller. It is therefore more time for close interactions, which possibly can cause capture. The asymmetry is most visible for Uranus and Neptune.

Figure 3.3 shows the relation between eccentricity and semi-major axis for each planet and for the simulation with all planets included. For all simulations, we see that all captured ISOs, end up with very eccentric orbits, where a majority of objects end up at $10^{-2} < e - 1 < 10^{-5}$. We also see a shift towards larger semi-major axis for captured ISOs, going from Jupiter to Neptune. Looking at all the simulations, the range for semi-major axis is from tens of au to 6.5×10^4 au (where our limit also is). This can also be seen in Fig. 3.2. In Fig. 3.3, one can also see that larger semi-major axis generally results in higher eccentricity. This relation has also been shown by Goulinski and Ribak (2017).

Plots showing the relation between perihelion distance and semi-major axis have also been done and can be seen in appendix B, Fig. B.2. These plots show that the perihelion distance for most captured ISOs varies between 10^{-1} and 10^2 au. However, for some ISOs, the perihelion distance is close to the radius of the Sun ($\sim 4.65 \times 10^{-3}$ au). This indicates that for the most eccentric orbits, there is a possibility that the ISO can collide with the Sun.

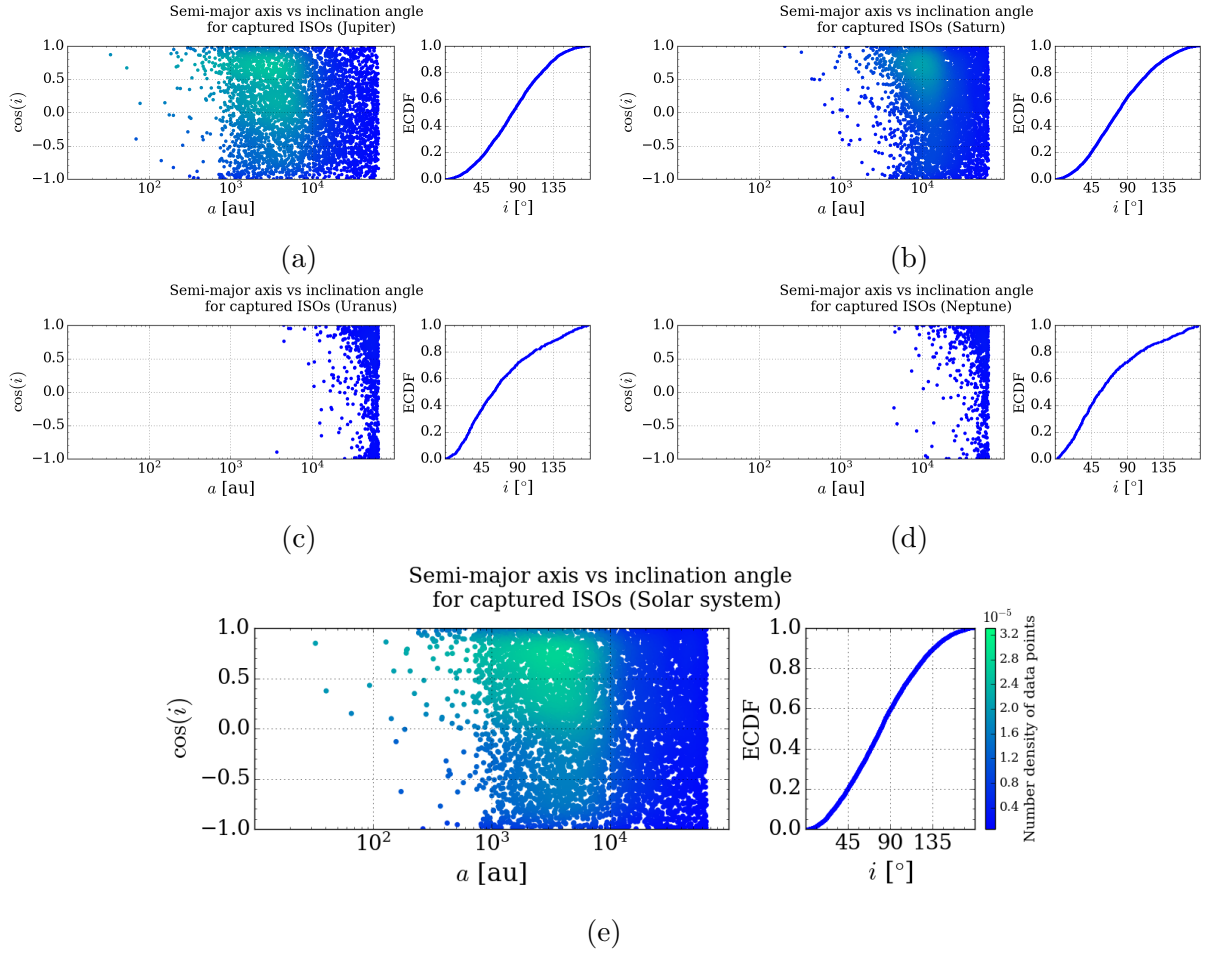

Figure 3.2: Plots showing semi-major axis versus inclination angle for captured ISOs in simulations with one planet and one simulation with all planets included. The ECDF for the inclination angle is also included for each plot. Lighter colour indicates higher number density (which is normalised and scaled such that it is comparable between the plots).

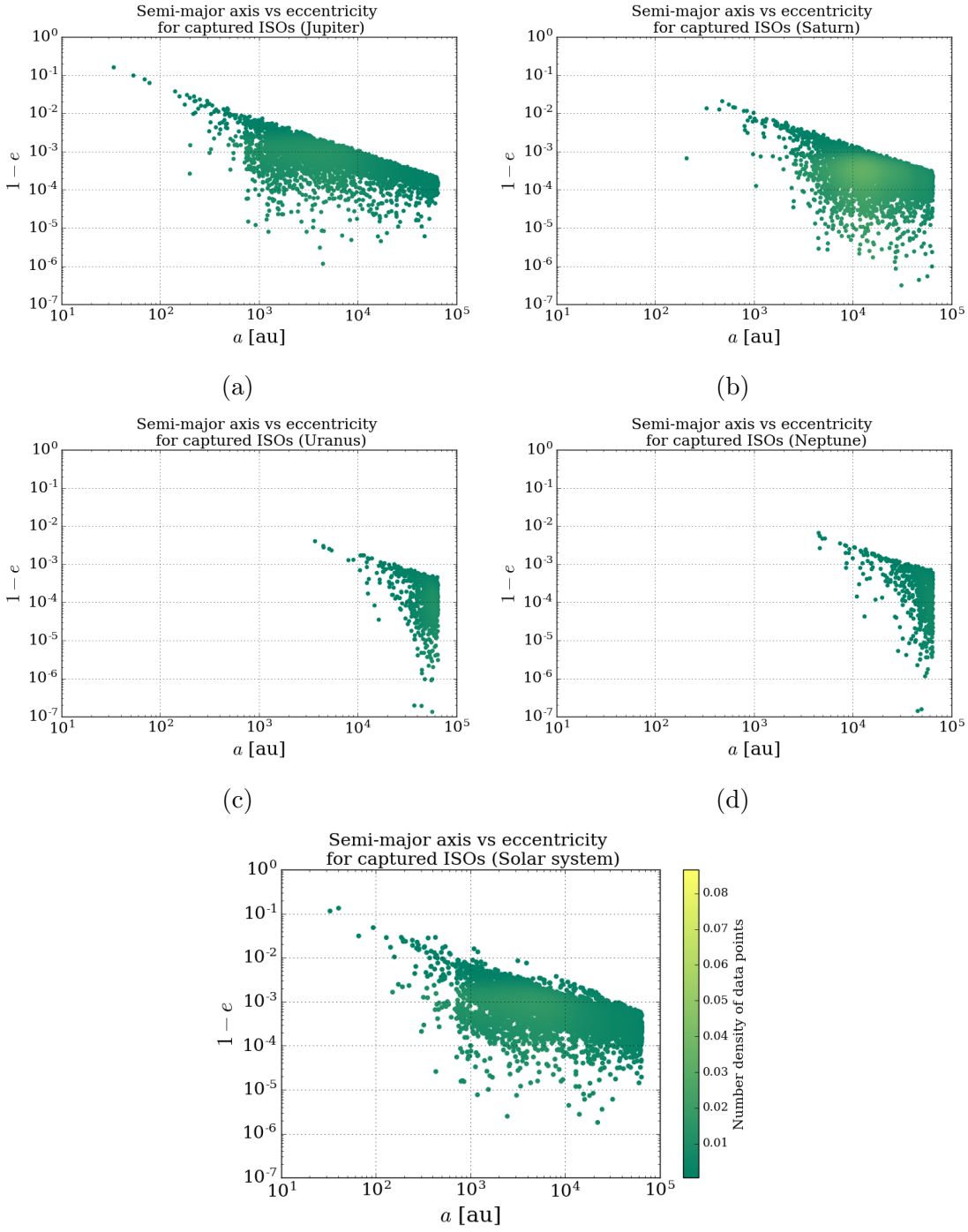

Figure 3.3: Plots showing semi-major axis versus eccentricity for captured ISOs in simulations with one planet and one simulation with all planets included. Lighter colour indicates higher number density (which is normalised and scaled such that it is comparable between the plots).

3.2 Close encounter with Jupiter

Following after the simulations where we study the contribution each planet has on the capture rate, a smaller set of simulations are done, of which the purpose is to study if a close encounter with a planet is necessary for capture. In this simulation, we have only considered Jupiter and fixed velocity at $v_\infty = 0.05$ km/s. We randomly select 10 ISOs that are captured in the previous simulation, but now reintegrate them with an output interval of a quarter of a year. This makes it possible to follow the change in position, velocity and orbital elements. The reason why this output interval is not used in the previous simulation with Jupiter, is because of the overwhelmingly amount of data that would made for 100,000 ISOs.

For MERCURY to register a close encounter, the ISO has to be within a specified distance to Jupiter. This distance is set to 30 Hill radii[1] (about 10 au), which ensures that most close encounters will be registered. To see if a close encounter is required for a capture, we calculate the total energy (kinetic and potential energy) per mass of the ISO and see how it change w.r.t time. We then see if the expected change in total energy (which should become negative when the ISO is captured) occurs at the same time when a close encounter happen.

The simulation shows that for all 10 ISOs, a change in total energy corresponds with a close encounter with Jupiter. A plot for one of the simulated ISOs, can be seen in Fig. 3.4, which shows the change in total energy per mass and the time when the close encounter with Jupiter occurs. A majority of the 10 ISOs resulted in similar plots to the one in Fig. 3.4, but a couple of plots also shows more than one close encounter with Jupiter. This can for example be seen in Fig. 3.5, which shows three close encounters with Jupiter, due to a relative short period of $\sim 10,000$ yr for the captured ISO.

Three different plots are included in the Fig. 3.5: top for the change in total energy per mass of the ISO, bottom left for how eccentricity change and bottom right for the Tisserand parameter (see below). From these plots one can see that a close encounter causes a change in both total energy and eccentricity, while the Tisserand parameter remains constant after an encounter with Jupiter.

The Tisserand parameter can be applied in the restricted three body problem, which in this case consists of the Sun, Jupiter and an ISO. The parameter can be calculated in the following way (Fitzpatrick 2016):

$$T_J = \frac{a_J}{a} + 2\cos(I)\sqrt{\frac{a}{a_J}(1-e^2)}, \tag{3.1}$$

where the variables I, inclination angle, e, eccentricity and a, semi-major axis, corresponds to the ISO, while a_J is the semi-major axis for Jupiter. The main feature of the Tisserand parameter is that it remains constant after close encounters with the planet in the three-body system, even though eccentricity and semi-major axis may change. In Fig. 3.5,

[1]The Hill radius is the radius of the so called Hill sphere, which is a region around a planet where the gravitational pull from the planet is larger then the one from the host star.

we see a small change in the Tisserand parameter in each close encounter, but overall, it remains constant. The Tisserand parameter can also be used to distinguish between comets, asteroids, and in our case, ISOs, since each object has its own unique value.

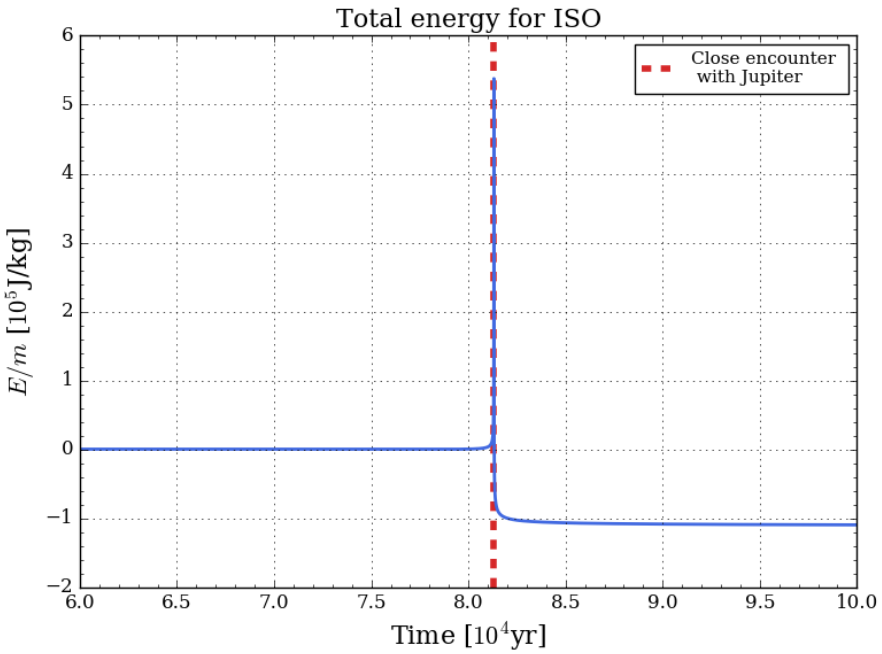

Figure 3.4: Plot showing the change in total energy per mass for one ISO and when it has a close encounter with Jupiter.

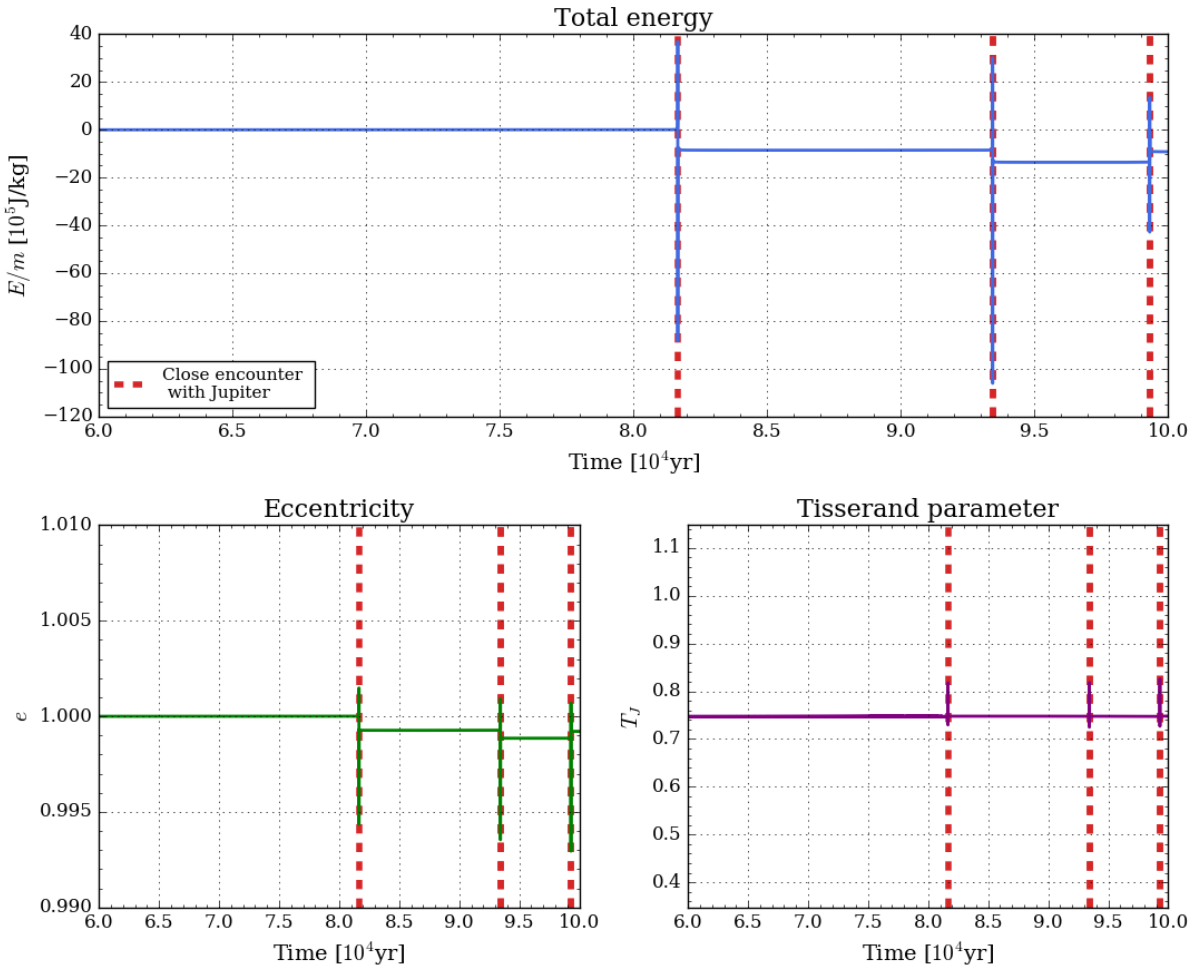

Figure 3.5: Three different plots for an ISO where several close encounters happen. Top for the change in total energy per mass of the ISO, bottom left for how eccentricity change and bottom right for the Tisserand parameter.

Chapter 4

Capture with four planets

The simulations made for deriving the total capture rate of interstellar objects (ISOs) are separated into four sets of simulations, where each set is a region in velocity at infinity between $0.05 - 16.0$ km/s (which was introduced in chapter 2, Tab. 2.1). The reason for splitting up the simulations has to do with integration time, which can be decreased for ISOs with higher initial velocity. However, the integration time is still chosen, such that the ISOs have enough time to reach the Solar system, and either get captured or flyby.

In all four sets, all of the giant planets, Jupiter, Saturn, Uranus and Neptune, are included. In total, 2,500,000 ISOs are simulated. The initial conditions for the ISOs are generated similarly as in section 3.1, with the main difference being that we now vary the initial velocity, as well as the value of $r_{\min}$. For the simulation with lowest initial velocities, we still have that $r_{\min} = 100$ au, but at 0.6-1.0 km/s, $r_{\min}$ is decreased to 70 au, and at $2.0 - 16.0$ km/s it is 50 au. This is because we expect the possibility for capture to decrease with higher velocity. We therefore limit the maximum impact parameter (Eq. 2.2) by decreasing the radius of the Solar system. However, we still follow the restriction which we introduced in section 3.1, i.e. the maximum impact parameter for captured ISOs should be $\lesssim 0.9 b_{\max}$, which is verified by test simulations. Details about the initial velocity for the ISOs, step size in velocity, choice of $r_{\min}$, integration time and number of ISOs simulated for each simulation, can be seen in Tab. 4.1.

Table 4.1: Table containing details about initial velocity for ISOs, what the step size in velocity is, what value $r_{\min}$ is when ISOs are generated, number of ISOs simulated and what the integration time is for each simulation.

	Simulation 1	Simulation 2	Simulation 3	Simulation 4
Velocity interval [km/s]:	0.05 - 0.5	0.6 - 1.0	2.0 - 6.0	8.0 - 16.0
Step size in velocity [km/s]:	0.05	0.1	1.0	2.0
Number of ISOs:	1,000,000	500,000	500,000	500,000
Integration time [yr]:	100,000	60,000	20,000	10,000
$r_{\min}$ [au]:	100	70	50	50

The conditions for an ISO to be considered captured are the same as in section 3.1, $e < 1$ and $a \leq 6.5 \times 10^4$ au. The Bootstrap method is once more used to calculate the fractional error of captured ISOs, and the calculation of the cross section at each initial velocity is also the same as in section 3.1, with Eq. 2.7. We also introduce a new parameter called volume capture rate per velocity step size: $Q/\mathrm{d}v$. This parameter is independent of the step size in velocity $\mathrm{d}v$, which we vary between different velocity regions. With this new parameter, we can compare capture rate between initial velocities v_∞. With Eq. 2.8 and 2.9, we define the volume capture rate per step size in velocity in the following way:

$$Q/\mathrm{d}v = v\sigma(v)f_{\mathcal{S}}(v), \tag{4.1}$$

where we assume that the velocity distribution $f_{\mathcal{S}}$, follows a Maxwellian distribution with a velocity dispersion of 30 km/s (Li and Adams 2015).

Figure 4.1 shows the volume capture rate per velocity step size versus initial velocity v_∞ (for a logarithmic y-scale, see appendix B, Fig. B.1). From Fig. 4.1, we can see that an initial velocity around $0.5 - 0.6$ km/s, results in the highest value of $Q/\mathrm{d}v$ and that it approaches zero at $v_\infty > 2$ km/s. The largest contribution to capture rate comes therefore from ISOs with $0.1 < v_\infty < 2$ km/s.

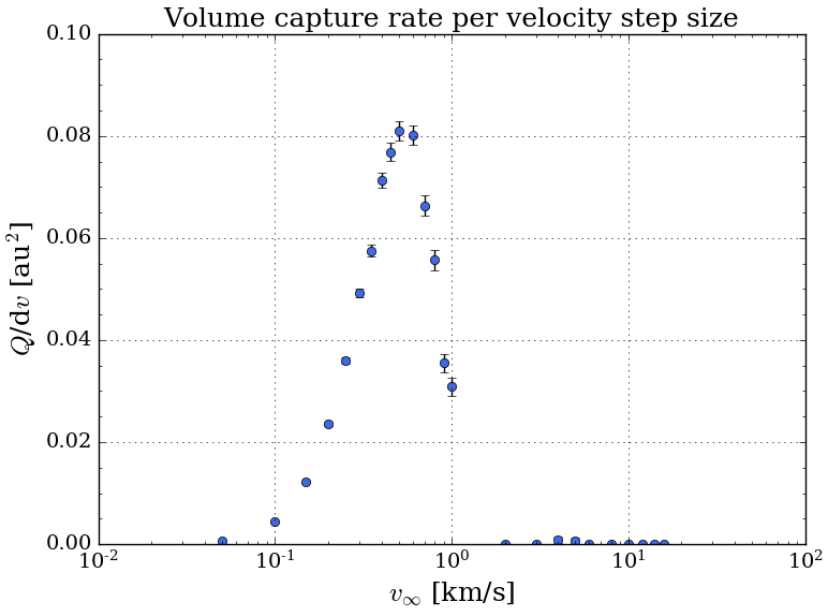

Figure 4.1: Plot showing the volume capture rate per step size in velocity for each initial velocity.

The calculation of the total volume capture rate is done the same way as in section 3.1, with the only difference that we now take the sum over all velocities. We still assume a Maxwellian distribution with a velocity dispersion of 30 km/s, and with the help of Eq. 2.8 and 2.9, we calculate the overall volume capture rate in the following way

$$Q = \sum_i v_i \sigma(v_i)(\mathrm{CDF}(v_i + \mathrm{d}v_i) - \mathrm{CDF}(v_i)), \tag{4.2}$$

where the CDF comes from the Maxwellian distribution. The overall volume capture rate for all simulated velocities is then calculated to be 0.0120(3) au^3/yr.

Orbital features for captured ISOs, such as semi-major axis versus eccentricity and inclination angle can be seen in Fig. 4.2 and 4.3. In Fig. 4.2, it is clear once again that the majority of captured ISOs end up with very eccentric orbits. One can also see a small favor towards lower eccentric orbits for ISOs with higher initial velocity, by looking at the difference in the empirical cumulative distribution function (ECDF).

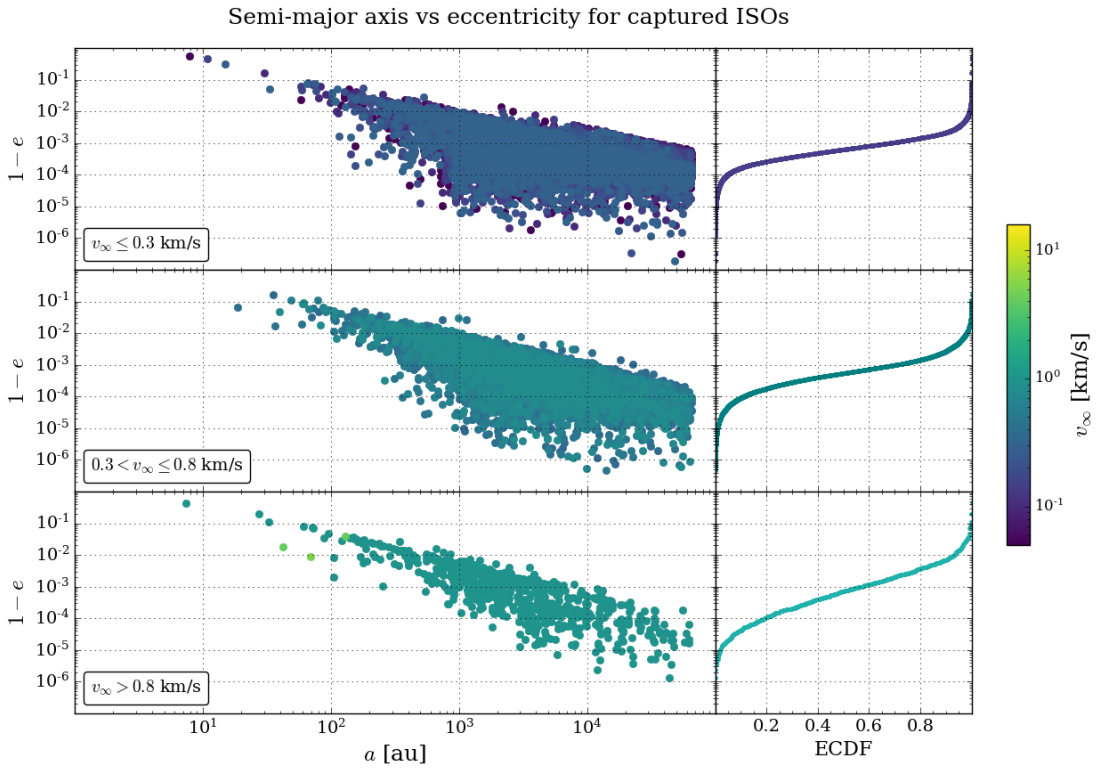

Figure 4.2: Plots showing the eccentricity versus semi-major axis for captured ISO and how it depends on initial velocity v_∞. The ECDF for $e - 1$ is also shown.

Figure 4.3 shows an asymmetry in the inclination angle (which was also shown in Fig. 3.2), where there are more captured ISOs with an inclination angle less than 90°. It is also shown with the help of ECDF, that this asymmetry is greater for ISOs with higher initial velocity v_∞.

Plots showing the ECDF for the semi-major axis of captured ISOs can be seen in Fig. 4.4. From these plots, one can see that ISOs with higher initial velocities slightly favor orbits with smaller semi-major axis. E.g., one can see that for captured objects with

$v_\infty > 0.8$ km/s, there is a higher per cent of captured objects with a semi-major axis equal to 10^3 au, compared to captured objects with $v_\infty \leq 0.8$ km/s.

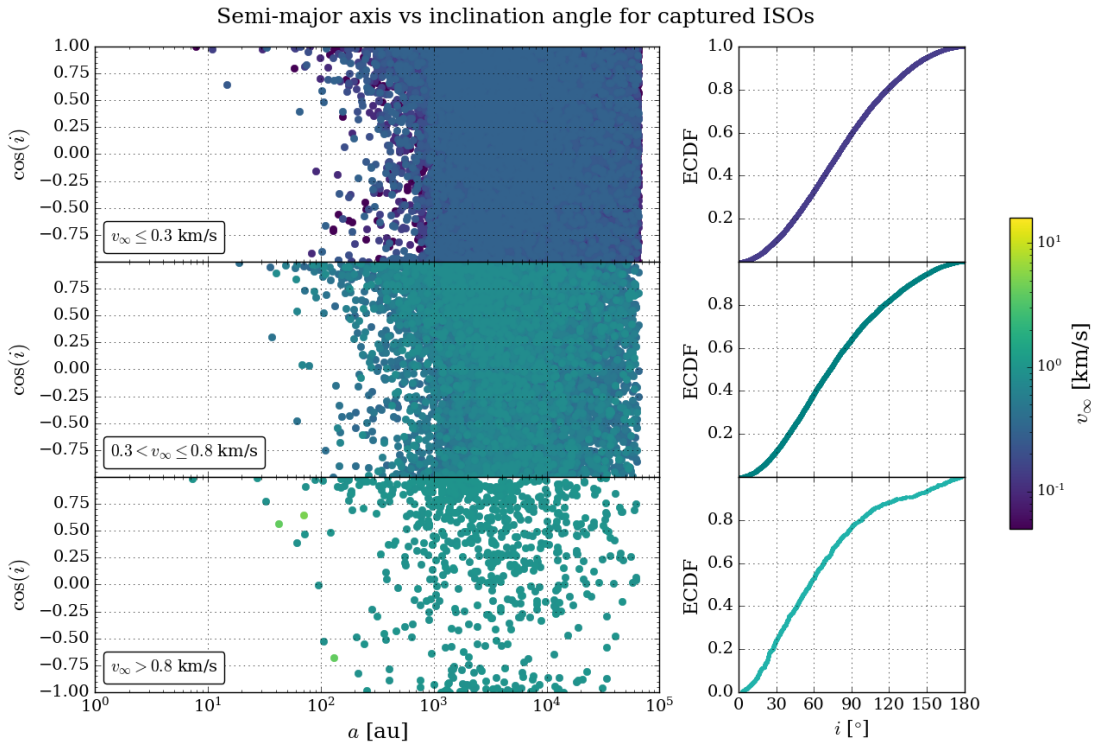

Figure 4.3: Plots showing the relation between inclination angle and semi-major axis for captured ISOs and how it depends on initial velocity. The ECDF for the inclination angle is also shown.

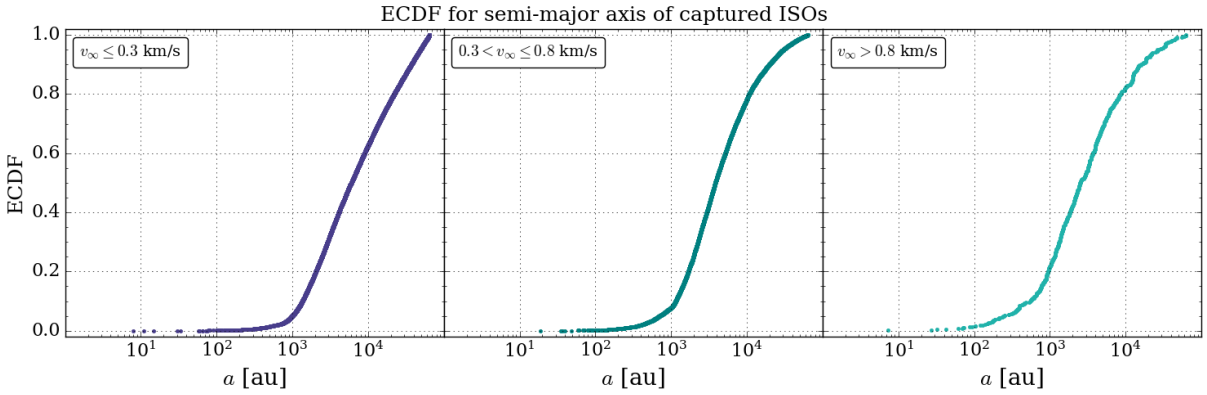

Figure 4.4: Plots showing the ECDF for semi-major axis of captured ISOs at different initial velocities.

Chapter 5

Long-term evolution

Even if an interstellar object gets captured, it may not be able to stay in the Solar system for very long due to potentially numerous close encounters with planets, which can cause ejections. This could for example be the cause for the difference in capture cross section of the Solar system and the sum of those for each individual planet (see section 3.1). To further understand this, we study the long-term evolution of 10 ISOs that were captured in the simulation with fixed $v_\infty = 0.05$ km/s, and all giant planets present (section 3.1). These 10 ISOs are randomly selected and are simulated once more, but this time with a integration time of 100 Myr and an output interval of 10^4 yr. This integration time may be enough to see if captured ISOs eventually get ejected with time. Here we set a maximum heliocentric distance beyond which the ISO is considered ejected. This limit is set to 10^5 au, which has been shown to be consistent with the most outer region in the Oort cloud (Correa-Otto and Calandra 2019). Close encounters with the planets are also registered and the set up of the simulation is the same as in section 3.2.

To study the possible effects long-term evolution has on a captured ISO's orbit, we look at the same parameters as in section 3.2. These are the total energy per mass, eccentricity and Tisserand parameter; all w.r.t. time. The Tisserand parameter is calculated w.r.t. Jupiter.

The simulation shows that all of the 10 captured ISOs are ejected within the integration time, where the majority of objects are ejected already after a few Myr. The cause of ejection is in all cases a close encounter with a planet (which we define the same way as in chapter 3: the object is within 30 hill radii to respective planet). However, how many close encounters there are in between capture and ejection, varies much. An example where just a few close encounters lead to an ejection can be seen in Fig. 5.1, which shows the total energy per mass, eccentricity and Tisserand parameter for one ISO. In this figure, we can see that at each close encounter there are instantaneous changes in the quantities, while in between, there are no such changes (which we also saw in section 3.2). After the ISO is captured, each encounter causes the total energy per mass and eccentricity to increase, until it is eventually ejected. We can also see that the Tisserand parameter, which we calculate w.r.t. Jupiter, no longer remains constant and both increases and decreases when the ISO encounters a different planet from Jupiter, which is expected. Another example where as

many as a few tens of close encounters occur between capture and ejection, can be seen in appendix B, Fig. B.3.

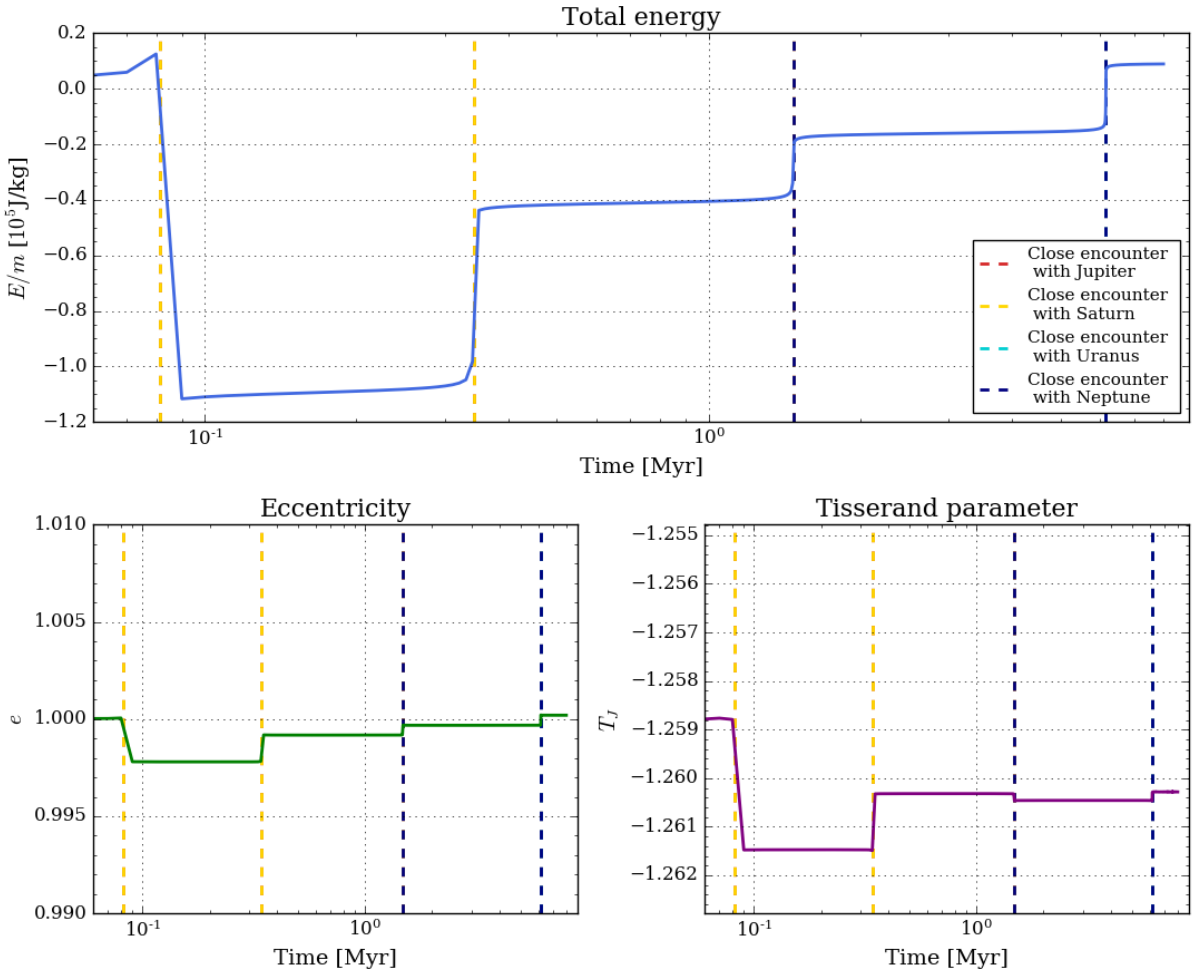

Figure 5.1: Long-term evolution for an ISO that gets ejected after just a few close encounters. Note: In some cases, close encounters between different planets happen within a relative short period of time, and only one coloured line is then visible. That is why close encounters with Jupiter and Uranus also are labelled.

Chapter 6

Discussion and conclusions

In chapter 3, the result regarding how a capture happens, indicates that it is very likely that a capture corresponds to a close encounter with a planet. This is because we can see that the time when the total energy per mass becomes negative (i.e. the ISO becomes bound to the Solar system) correlates well with the time when the ISO is close to Jupiter. When we studied the long-term evolution for captured ISOs (see chapter 5), we saw changes in total energy per mass and eccentricity for each close encounter, and eventually, after a few Myr, the ISO gets ejected out from the Solar system. With these two results, it is very likely that close encounters with planets can result in both capture and ejection. However, the result also implies that there is a large variation in number of close encounters between capture and ejection. We can therefore only say that close encounters most likely is significant for capture and ejection, but what exactly happens during an encounter (e.g. the trajectories of the objects) remains to be explored.

The contribution each planet has on the capture rate (see chapter 3), seems to not be additive, since the result implies that the the cross section for the Solar system is less than the sum of the cross section for each individual planet. An explanation for this may be that the probability for close encounters increases with more planets included. Since our results suggest that close encounters also can cause ejections, it is likely that an ISOs that would be captured with only one planet present, can get ejected by a second close encounter with a different planet. However, despite this, it is clear that when all planets are included, the capture rate is clearly increased compared to when only one planet is present, which was highlighted by Hands and Dehnen (2020) for ISOs at $v_\infty \leq 0.5$ km/s.

In chapter 4, we looked at the capture rate for ISOs with varying initial velocities between $0.05 - 16.0$ km/s following a Maxwellian distribution, in a Solar system consisting of the four giant planets. The result indicates a volume capture rate of 0.0120(3) au^3/yr, and if we assume a number density of 0.1 au^{-3} for 'Oumuamua-like objects (Meech et al. 2017), we get a capture rate of 1200(30) Myr^{-1}. The result also suggests that it is more likely to capture an object at $0.5 - 0.6$ km/s, since the capture rate is relative high and the number density of these object also is relatively high, which also was found by Hands and Dehnen (2020).

Comparing our value of the volume capture rate, 0.0120(3) au^3/yr, with the value

derived by Hands and Dehnen (2020), 0.051 au^3/yr, who only considered Jupiter in their simulations and used a slightly different methodology, our value is less than a quarter, but within the same order of magnitude. From our comparison of capture rate between one planet and all four planets present (chapter 3), we saw that when $v_\infty = 0.05$ km/s, the volume capture rate is larger when all of the giant planets are included, compared to when only Jupiter is considered. From this, one can suspect that our value of the volume capture rate is lower than expected. This may be due to the sudden drop in $Q/\mathrm{d}v$ in Fig. 4.1, where the contribution from the majority of ISOs at $v_\infty > 1$ becomes zero, since no captures happen. The reason why no captures happen may be due to the number of simulated ISOs, which is 100,000 ISOs per unit velocity. This gives an accuracy of 10^{-5}, which may not be enough since we expect the probability for capture to decrease with velocity. An improvement for future work is therefore to increase the number of simulated ISOs at higher velocities.

The orbital features of captured ISOs in the presence of different planets which we looked at in chapter 3, indicates that when we go from Jupiter to Neptune, the semi-major axis for captured ISOs increases (see Fig. 3.3 and 3.2). One can then speculate that this is due to the difference in gravity, where Jupiter has a much larger gravitational pull, which perhaps can result in orbits of lower binding energy and therefore smaller semi-major axis. An asymmetry in inclination angle has also been observed, where there are more captured ISOs with an inclination smaller than 90°, in agreement with Hands and Dehnen (2020) and Goulinski and Ribak (2017). In chapter 4, we also saw minor indications that captured ISOs with higher initial velocity, result in less eccentric orbits with smaller semi-major axis. However, since the reason is not clear, and that the indication is very small, further investigation is needed.

An improvement regarding if a close encounter is necessary for capture, is to increase the sample size. The same holds for the long-term evolution of captured ISOs. With only 10 ISOs propagated in both cases, we are suffering from small number statistics. So in the future, more intensive simulations are needed. The importance with larger sample sizes is also highlighted by the fact that the time period between capture and ejection, which in our case is a few Myr, differ from the 10 Myr time period suggested by Hands and Dehnen (2020).

We suggest studying how a capture or ejection of ISOs happen in more detail than what has been done in this thesis. We also call for a more detailed study on the Tisserand parameter, which we only briefly touched upon in this project. Perhaps it can be used to identify objects with interstellar origin in the Solar system, by comparing the value of the Tisserand parameter with values of simulated ISOs. Recent research indicates that high-inclination Centaurs in the Solar system probably has a interstellar origin (Namouni and Morais 2020). It is therefore interesting to see if other objects in the Solar system could potentially be captured ISOs, and the Tisserand parameter can then potentially be an additional method.

In conclusion, through N-body simulations, in which we include the giant planets Jupiter, Saturn, Uranus and Neptune, we have derived a volume capture rate of 0.0120(3) au^3/yr for capture of ISOs in the Solar system. For ISOs with low initial velocity ($v_\infty = 0.05$

km/s) the result indicates that the contribution on capture rate for each planet is not additive, due to the increase in number of close encounters with planets, which can cause ejections. However, the simulation that results in highest capture rate is still the one with all four planets included. The result also suggest that it is most likely ISOs with velocity at infinity $0.5 - 0.6$ km/s and inclination angle smaller than $90°$, that are to be captured by the Solar system, and that the orbit for captured ISOs usually is very eccentric with large semi-major axis. Finally, for a capture to happen, it is most likely that a close encounter with a planet is necessary. A captured ISO may then be subject to subsequent encounters with the planet(s) and are then typically ejected in a few Myr.

Bibliography

Chambers, J. E. (1999). A hybrid symplectic integrator that permits close encounters between massive bodies. *Monthly Notices of the Royal Astronomical Society*, 304(4):793–799.

Correa-Otto, J. A. and Calandra, M. F. (2019). Stability in the most external region of the Oort Cloud: evolution of the ejected comets. *Monthly Notices of the Royal Astronomical Society*, 490(2):2495–2506.

Engelhardt, T., Jedicke, R., Vereš, P., Fitzsimmons, A., Denneau, L., Beshore, E., and Meinke, B. (2017). An Observational Upper Limit on the Interstellar Number Density of Asteroids and Comets. *AJ*, 153(3):133.

Fitzpatrick, R. (2016). Three-body problem. `https://farside.ph.utexas.edu/teaching/celestial/Celestial/node78.html`.

Goulinski, N. and Ribak, E. N. (2017). Capture of free-floating planets by planetary systems. *Monthly Notices of the Royal Astronomical Society*, 473(2):1589–1595.

Hands, T. O. and Dehnen, W. (2020). Capture of interstellar objects: a source of long-period comets. *Monthly Notices of the Royal Astronomical Society: Letters*, 493(1):L59–L64.

Jackson, A. P., Tamayo, D., Hammond, N., Ali-Dib, M., and Rein, H. (2018). Ejection of rocky and icy material from binary star systems: implications for the origin and composition of 1I/'Oumuamua. *MNRAS*, 478(1):L49–L53.

Jewitt, D. and Luu, J. (2019). Initial characterization of interstellar comet 2i/2019 q4 (borisov). *The Astrophysical Journal*, 886(2):L29.

JPL's Solar System Dynamics group (2017). JPL Small-Body Database Browser. `https://ssd.jpl.nasa.gov/sbdb.cgi?sstr=%27Oumuamua;old=0;orb=0;cov=0;log=0;cad=0#elem`.

Li, G. and Adams, F. C. (2015). Cross-sections for planetary systems interacting with passing stars and binaries. *Monthly Notices of the Royal Astronomical Society*, 448(1):344–363.

McGlynn, T. A. and Chapman, R. D. (1989). On the Nondetection of Extrasolar Comets. *ApJ*, 346:L105.

McMillan, S. L. W. and Hut, P. (1996). Binary–Single-Star Scattering. VI. Automatic Determination of Interaction Cross Sections. *ApJ*, 467:348.

Meech, K. J., Weryk, R., Micheli, M., Kleyna, J. T., Hainaut, O. R., Jedicke, R., Wainscoat, R. J., Chambers, K. C., Keane, J. V., Petric, A., Denneau, L., Magnier, E., Berger, T., Huber, M. E., Flewelling, H., Waters, C., Schunova-Lilly, E., and Chastel, S. (2017). A brief visit from a red and extremely elongated interstellar asteroid. *Nature*, 552(7685):378–381.

Meech, K. J., Yang, B., Kleyna, J., Hainaut, O. R., Berdyugina, S., Keane, J. V., Micheli, M., Morbidelli, A. r., and Wainscoat, R. J. (2016). Inner solar system material discovered in the Oort cloud. *Science Advances*, 2:e1600038.

Micheli, M., Farnocchia, D., Meech, K. J., Buie, M. W., Hainaut, O. R., Prialnik, D., Schörghofer, N., Weaver, H. A., Chodas, P. W., Kleyna, J. T., Weryk, R., Wainscoat, R. J., Ebeling, H., Keane, J. V., Chambers, K. C., Koschny, D., and Petropoulos, A. E. (2018). Non-gravitational acceleration in the trajectory of 1I/2017 U1 ('Oumuamua). *Nature*, 559:223–226.

Namouni, F. and Morais, M. H. M. (2020). An interstellar origin for high-inclination Centaurs. *MNRAS*, 494(2):2191–2199.

'Oumuamua ISSI Team, Bannister, M. T., Bhand are, A., Dybczyński, P. A., Fitzsimmons, A., Guilbert-Lepoutre, A., Jedicke, R., Knight, Matthew M., M. K. J., McNeill, A., Pfalzner, S., Raymond, S. N., Snodgrass, C., Trilling, D. E., and Ye, Q. (2019). The natural history of 'Oumuamua. *Nature Astronomy*, 3:594–602.

Pfalzner, S. and Bannister, M. T. (2019). A hypothesis for the rapid formation of planets. *The Astrophysical Journal*, 874(2):L34.

Raymond, S. N., Armitage, P. J., and Gorelick, N. (2010). Planet-Planet Scattering in Planetesimal Disks. II. Predictions for Outer Extrasolar Planetary Systems. *ApJ*, 711(2):772–795.

Trilling, D. E., Mommert, M., Hora, J. L., Farnocchia, D., Chodas, P., Giorgini, J., Smith, H. A., Carey, S., Lisse, C. M., Werner, M., McNeill, A., Chesley, S. R., Emery, J. P., Fazio, G., Fernandez, Y. R., Harris, A., Marengo, M., Mueller, M., Roegge, A., Smith, N., Weaver, H. A., Meech, K., and Micheli, M. (2018). Spitzer Observations of Interstellar Object 1I/'Oumuamua. *AJ*, 156(6):261.

Yen, L. (2019). An introduction to the bootstrap method. `https://towardsdatascience.com/an-introduction-to-the-bootstrap-method-58bcb51b4d60`.

Appendix A

Bootstrap method

To calculate the probability for a capture to happen, one can simply divide the number of captured objects with the total number of objects. The big downside with this is that an error estimate is left out. In this project, we will therefore use a method called Bootstrap, which makes it possible to get a error estimate for the probability of a capture (Yen 2019).

Bootstrap is a widely used statistical method applied in a variety of areas. It is based on resampling and sampling with replacement and to illustrate this, let us assume we have known sample with sample size n. We can then draw a sample with a size free of choice from the original sample; this is the so called resampling. How we draw these samples is with replacement, which means that when a element is drawn, it goes back into the original sample, making it possible to draw the same element several times.

This resampling can be replicated B number of times, resulting in a total of B Bootstrap samples. For each Bootstrap sample, an estimate/calculation can be done. In our case, this estimate/calculation is the probability for capture. This results in B number of estimates, from which a mean value and variance can be calculated from. The standard error for our estimate is then the square root of the variance. Both the mean value and the variance converges to their respective true value when we let $B \to \infty$. With the help of computers, we can choose B such that we get a valid approximation for the mean value and variance.

Appendix B

Additional plots

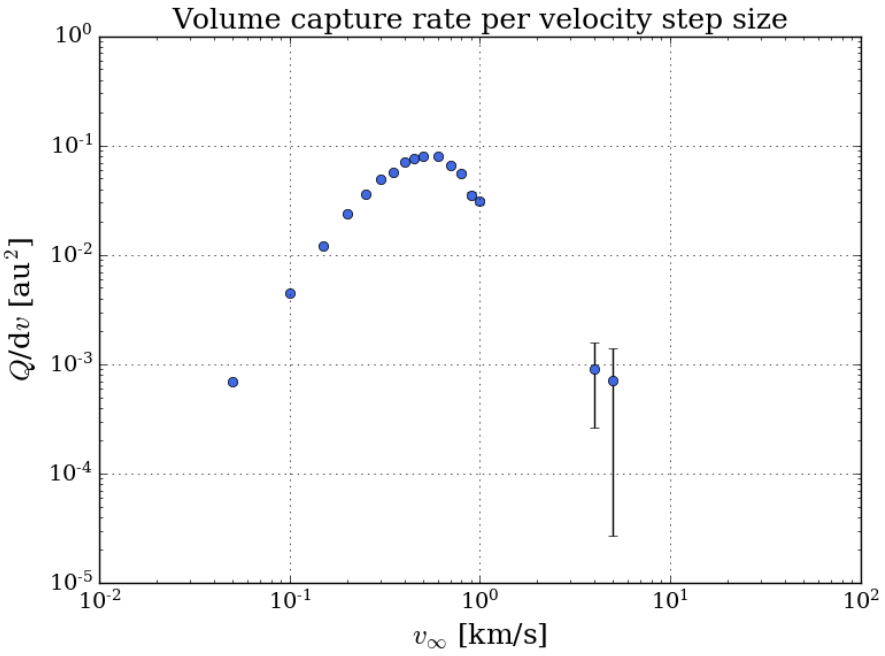

Figure B.1: Volume capture rate per step size in velocity for each initial velocity. Due to a logarithmic scale on the y-axis, those points with $Q/\mathrm{d}v = 0$ au^2, is not shown.

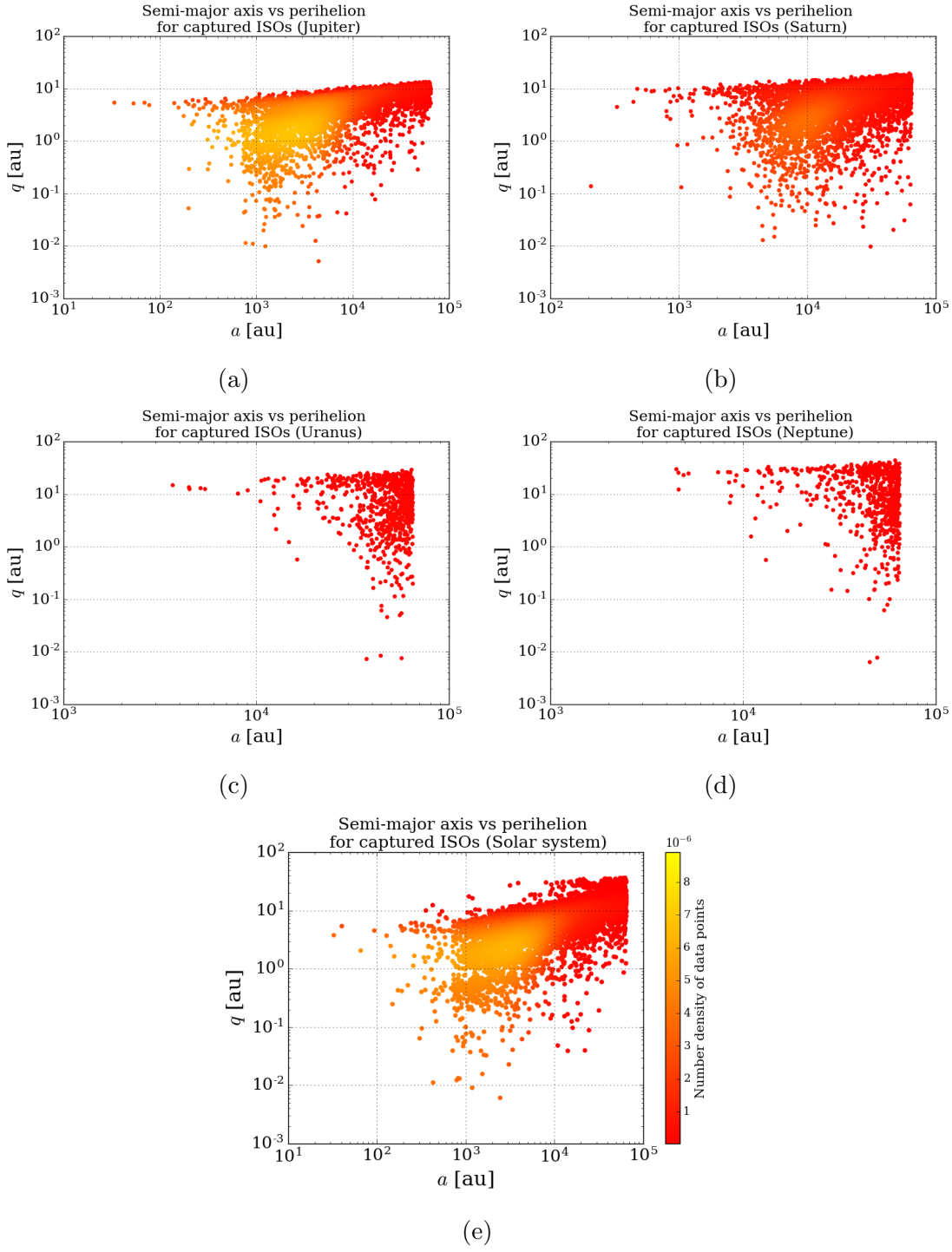

Figure B.2: Plots showing semi-major axis versus perihelion distance for captured ISOs in simulations with one planet and one simulation with all planets included. Lighter colour indicates higher number density (which is normalised and scaled such that it is comparable between the plots).

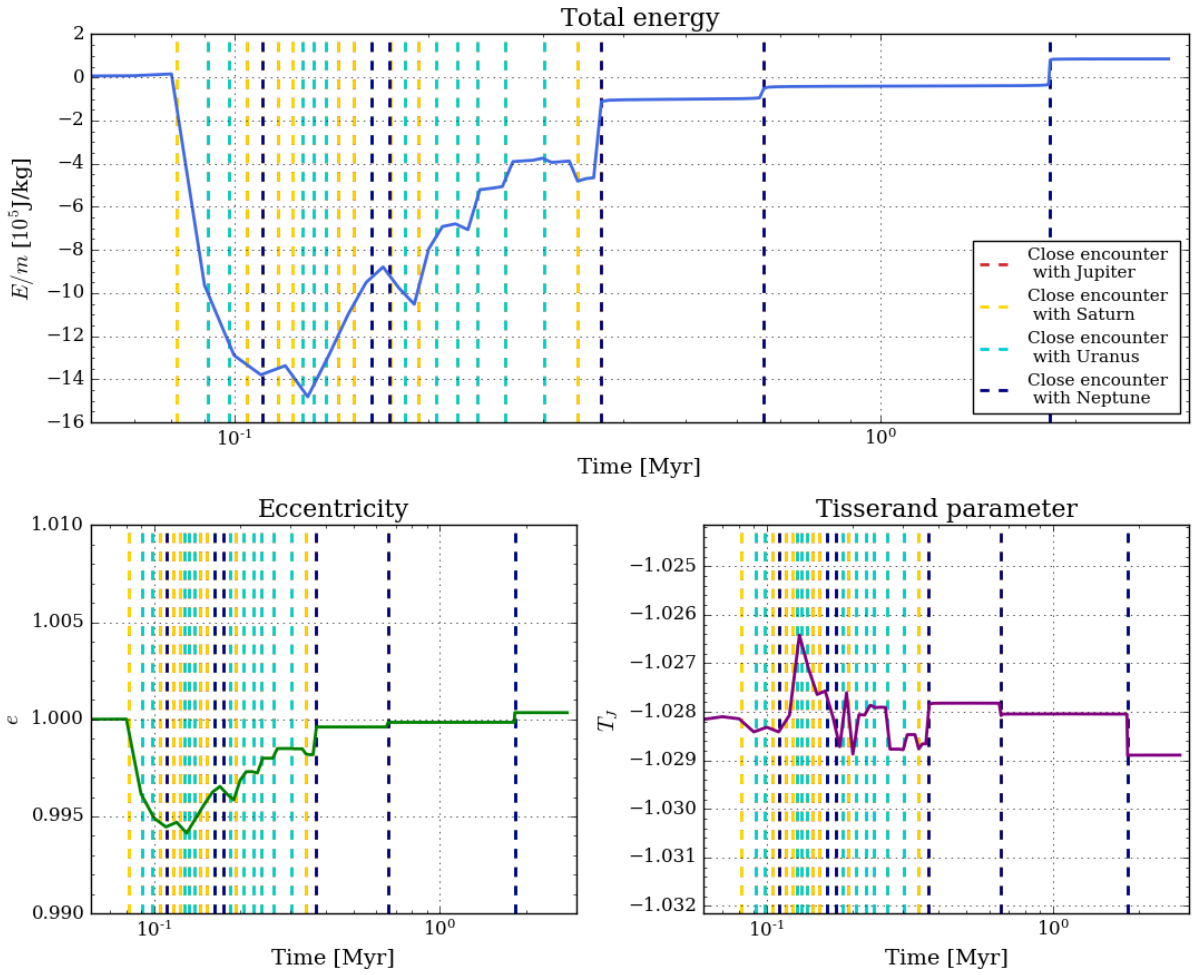

Figure B.3: Long-term evolution for an ISO that eventually gets ejected after as many as a few tens of close encounters.